

Brief communication: Sharp ~~winter~~ precipitation ~~transition~~ gradient on the southern edge of the Tibetan Plateau during cold season

Titouan Biget¹, Fanny Brun¹, Walter Immerzeel², Léo Martin³, Hamish Pritchard⁴, Emily Collier⁵, Yanbin Lei^{6,7}, and Tandong Yao^{6,7}

¹Université Grenoble Alpes, CNRS, INRAE, IRD, Grenoble INP, IGE, 38400 Saint-Martin-d'Hères, France

²Department of Physical Geography, Utrecht University, Utrecht, The Netherlands

³Aix Marseille Univ, CNRS, IRD, INRAE, CEREGE, Aix-en-Provence, France

⁴British Antarctic Survey, Cambridge, United Kingdom

⁵Department of Atmospheric and Cryospheric Sciences (ACINN), University of Innsbruck, Innrain 52, Innsbruck, 6020, Austria

⁶Key Laboratory of Tibetan Environment Changes and Land Surface Processes, Institute of Tibetan Plateau Research, Chinese Academy of Sciences, Beijing 100101, China

⁷CAS Center for Excellence in Tibetan Plateau Earth System Sciences, Beijing, 100101, China

Correspondence: Titouan Biget (titouan.bgt@gmail.com)

Abstract.

The Tibetan Plateau is a high-altitude arid region, where limited in-situ precipitation measurements are available. In this communication, we document a strong precipitation gradient at the southern edge of the Paiku Co catchment (southern Tibetan Plateau) from in-situ data and atmospheric model outputs. In particular, we use water pressure time series from proglacial lakes, two automatic weather stations, and data from ERA5-Land reanalysis and CORDEX-FPS-CPTP ensemble. We show that precipitation totals can vary by one order of magnitude over a short distance of 10 km in a rather smooth terrain ~~throughout the winter and the pre-monsoon~~ during the cold season. This large precipitation ~~gradients~~ gradient marks the transition between the great Himalayas and the Tibetan Plateau.

Copyright statement. TEXT

10 1 Introduction

The Tibetan Plateau is a high-altitude region characterized by a dry and arid climate, and by the presence of multiple lakes and glaciers (Yang et al., 2014). Most of the lakes of the Tibetan Plateau have been expanding rapidly since the mid-1990s, representing an additional terrestrial water storage of 6 to 9 Gt yr⁻¹ (Zhang et al., 2017). However, some lakes located on the southern edge of the plateau have shrunk for the last three decades (Lei et al., 2018; Zhang et al., 2021). The changes in lake volume are mostly attributed to decadal changes in precipitation (Zhang et al., 2021). Precipitation measurements are scarce on the Tibetan Plateau, and thus analysis of climate and meteorology relies largely on reanalysis, remote sensing products, and climate models (e.g., Collier et al., 2024).

The challenges associated with precipitation measurements are numerous in mountainous regions, especially when a substantial fraction falls in solid forms. Precipitation gauges suffer from large underestimations of solid precipitation, 42.6% on average for unshielded gauges and 30.6% for single-Alder shielded gauges (Kochendorfer et al., 2017). These underestimations can be much larger in cases of strong winds (Goodison et al., 1998). To overcome these issues, recent studies suggested that solid precipitation could be also estimated from frozen lake [water](#) pressure changes (Pritchard et al., 2021). This method relies on the assumption that the catchment is frozen, making the surface run-off and the evaporation negligible due to the cold conditions. Since lakes are used as sensors, the size of the sensor is 6 to 9 orders of magnitude above the size of common precipitation gauges, thus providing a spatially averaged estimate of precipitation that is expected to be less sensitive to undercatch and to spatial variability of precipitation (Pritchard et al., 2021), at the cost of application over only a few months of the year.

In this study, we report new observations of lake level changes during the cold season (December to May) of a catchment located on the southern edge of the Tibetan Plateau. From the lake water pressure time series, we reconstruct precipitation estimates based on Pritchard et al. (2021)'s method and compare them to conventional gauge measurements located on both sides of the orographic barrier of the Himalaya. We then compare these observations to precipitation estimates from two datasets, ERA5-Land reanalysis (Copernicus Climate Change Service) and simulations from the Coordinated Regional Climate Downscaling Experiment Flagship Pilot Study (CORDEX-FPS) Convection-Permitting Third Pole (CPTP) project (Collier et al., 2024; Prein et al., 2023), to discuss the added value of kilometer-scale convection-permitting atmospheric models.

2 Study site

The in-situ measurements were collected in the southern part of the endorheic Paiku basin (Fig. 1 - a), on the southern Tibetan Plateau (China). The catchment drains into Paiku Co, an alpine lake situated at 4590 m a.s.l. that has an area of approximately 270 km², which is slightly more than one tenth of the whole catchment (2376 km²). Paiku Co is partially fed by the 41 glaciers present in the basin (Lei et al., 2018). Although Paiku Co lake has shrunk for the last decades, proglacial lakes located higher up in the catchment have been growing for the past 50 years due to glacier retreat (Lei et al., 2018).

We focus on the proglacial lake named Golojang Co, which is located in the south of the catchment at an elevation of 5357 m a.s.l and has an area of 5.54 km²(see Fig. 1 - a). It is frozen a large part of the year, during winter (DJF), pre-monsoon (MAM) and part of monsoon (starting in June), to finally break-up around July. The outlet of the lake flows through a moraine, then channels into the Nijile river. The lake occupies the over-deepening carved by the glacier retreat. The glaciers are still in contact with the lake, with a calving front releasing small icebergs. The surrounding orography may favor the accumulation of snow on its local lowest areas, i.e, on the frozen surface of the lake.

In Paiku Co catchment, for elevations below 5000 m a.s.l, the measured annual precipitation varies between 150 and 300 mm, with winter precipitation accounting for approximately 10% of the annual total (Lei et al., 2018, 2021; Martin et al., 2023). These estimates are based on an automatic weather station (AWS) located close to the main lake Paiku Co (at 4600 m a.s.l.; Lei et al., 2018), and an other AWS located 10 km south of the lake (named Paiku AWS in this study and located at 5030 m a.s.l.; Martin et al., 2023).

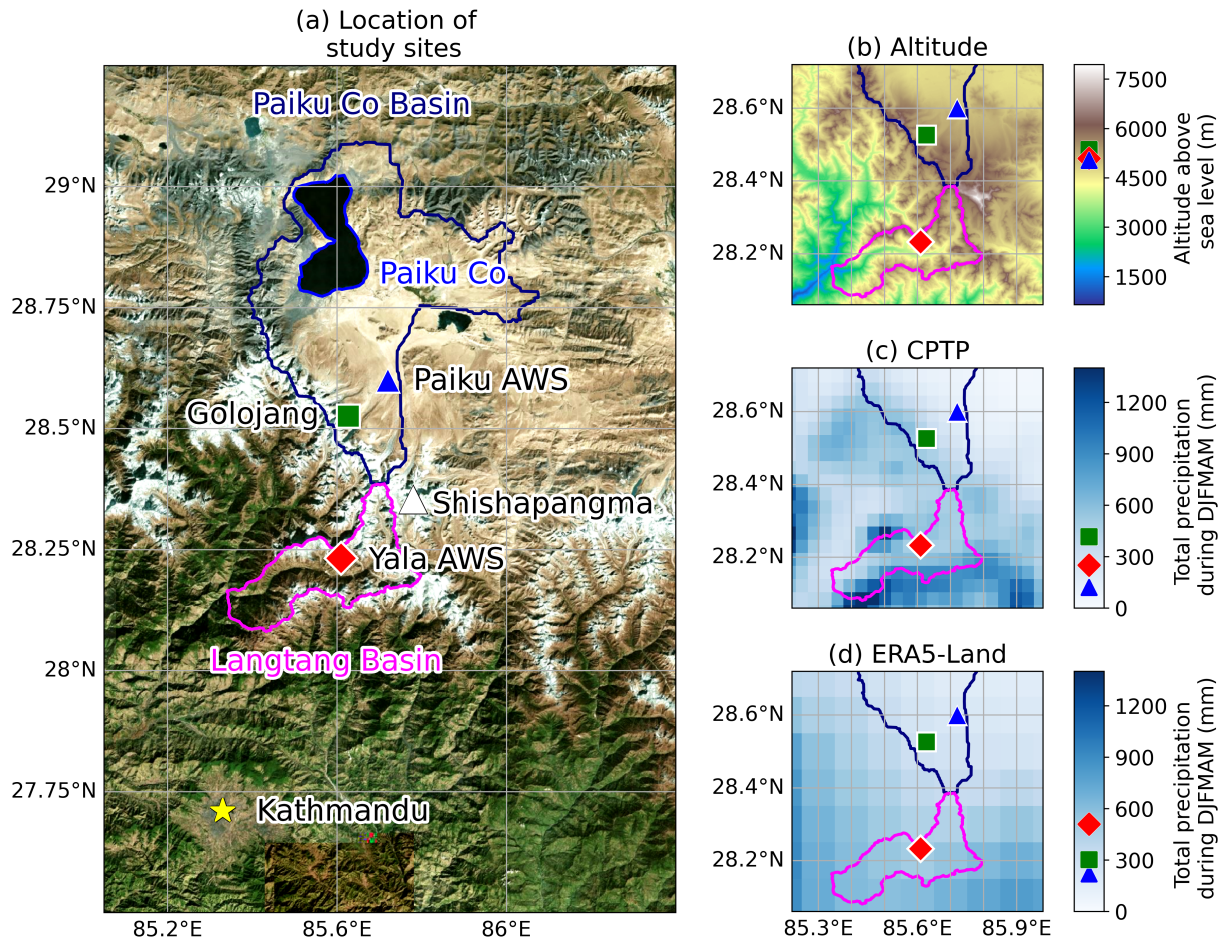


Figure 1. (a) Location of study sites. (b) Elevation and (c & d) spatial distribution of total precipitation above over the studied study area for from CPTP and ERA5-Land models from October 5 december 2019 to May 2022. The 15 July 2020. On the maps, the symbols represent show the locations of the in-situ recordings. On the color bars on the right side of the maps and their, symbols indicate interpolated values on of precipitation at the color bars study sites. The southernmost and brightest line marks solid lines mark the boundary of the Langtang National Park. The northernmost and darkest line marks the boundary Paiku Co basin.

3 Data and method

To estimate the precipitation around Paiku Co catchment, we use a collection of datasets from in-situ observations and from models.

3.1 Precipitation from meteorological stations

55 We use meteorological data from two AWS located on different sides of the Himalayas: on the northern side, within Paiku Co catchment in China, we use the Paiku AWS (5033 m a.s.l., Martin et al., 2023), and on the southern side, we use Yala AWS (5090 m a.s.l., Immerzeel et al., 2014) located in Langtang National Park in Nepal (Fig. 1 - a), near Yala Peak, base camp.

Both AWS record standard meteorological variables (air temperature and relative humidity, wind speed, incoming and outgoing radiation, and atmospheric pressure). Additionally, they measure snow thickness with a Campbell SR50 ultrasonic ranging sensor and precipitation with an OTT Pluvio2 all-weather precipitation gauge. Paiku Co AWS started recording from 29 October 2019, and the record is uninterrupted until May 2022. Antifreeze liquid and engine oil were added to the OTT Pluvio2 bucket in order to prevent the water inside it from freezing or evaporating. Yala AWS has been operating since October 2015 but was not recording from 18 November 2019 to 27 March 2020 due to data overwriting. The record is then uninterrupted until May 2022. Antifreeze was added to the OTT Pluvio2 bucket, but no oil was added, and thus evaporation is expected. 65 As a consequence, the signal from the precipitation gauge was rectified by replacing the decreasing height values with neutral values (not decreasing nor increasing). Both OTT Pluvio2 are equipped with a windshield.

3.2 Precipitation from lake water pressure

Three Hobo U20 [water](#) pressure transducers (PT) were immersed in Golojang Co and were recording from 01 November 2019 to 14 April 2022. A fourth PT placed outside the lake is used as an atmospheric pressure reference in order to correct for diurnal 70 changes in atmospheric pressure. The immersed PT record water pressure and temperature of the lake every half an hour. The PT were immersed at water depths ranging from 50 to 80 cm and hence could be frozen during the coldest months. Only one PT was never frozen, and consequently we analyze results from this single sensor. Because of the strong noise on the signal from the PT, we filter the series with a 48-hour rolling mean.

It has been demonstrated that such [water](#) pressure time series can be interpreted as direct measurements of the precipitation 75 falling onto the lake during winter-like conditions (Pritchard et al., 2021). This method relies on the assumption that the surface and sub-surface runoffs are at their minimum due to freezing conditions, and limited evaporation from the lake due to its ice cover, although it does not have to be necessarily entirely frozen if the evaporation is neglected. In these conditions, pressure variations in the lake are attributed only to the precipitation over the surface of the lake and its drainage. The typical pressure signal expected is a constant slow decrease due to the drainage of the lake, with some quick jumps due to precipitation. We used 80 two criteria to verify the frozen assumption: i- we extrapolate the temperature from Paiku AWS to the elevation of Golojang Co, assuming an -6.5 K/km environmental lapse rate, and keep days with a mean temperature below 0°C; and ii- we map the ice cover extent of Golojang Co from Landsat 7, 8, and Sentinel-2 images using the Google Earth Engine Digitisation Tool (GEEDiT; Lea, 2018) and keep periods with more than 90% of the surface frozen.

We followed the method developed by Pritchard et al. (2021) to estimate the precipitation amount over Golojang Co. When 85 the lake is frozen, the pressure measured by the PT sensor (p in Pa) follows the hydrostatic equation:

$$p = \rho_w g (h_w + h_{swe}) + p_0 \quad (1)$$

with ρ_w (in kg m^{-3}) being the density of liquid water, g (in m s^{-2}) being the acceleration of gravity, h_w (in m) the depth of the sensor relative to surface, h_{swe} (in m) being the water equivalent height of the snow and ice above the surface, and p_0 (in Pa) being an arbitrary constant. We assume that, at the time scale of a snowfall event (from a few hours to four days), changes in p (named dp) are solely due to changes in h_{swe} (named dh_{swe}), due to precipitation and to changes in h_w due to the lake drainage (named dh_w). Following Pritchard et al. (2021), we assume a constant drainage that is estimated by extrapolating p just before and after the event using a linear regression on the time series fitted with a least square method. The date of the beginning, the date of the ending, and the duration of the extrapolation were determined manually. For the rest of the study, we express changes in the total water column (dh in m) as:

$$95 \quad dh = \frac{dp}{\rho_w g} = dh_w + dh_{swe} \quad (2)$$

We assume that the uncertainty ε_{swe} on the measurement of precipitation during an event is the sum of ε_{D1} and ε_{D2} , which are respectively the uncertainties on the regression on the drainage before and after the snowfall. The uncertainty arising from the drifting of the PT is neglected since we estimated that the drifting is small enough to be considered as a systematic bias on the scale of a single event.

100 3.3 Precipitation from atmospheric models

We use daily precipitation from the CORDEX-FPS CPTP project (Collier et al., 2024) and from ERA5-Land (Muñoz Sabater et al., 2021). The former dataset consists of simulations from 13 different models or model configurations driven by ERA5 for the hydrological year of October 2019 to September 2020 using grid spacings ranging from 2.2 to 4 km. We used model output reprojected on homogeneous grids (approximately 4 km). We use the averages on the total daily precipitation from the 13 ensemble members. ERA5-Land variables are provided on an approximately 10 km grid. We use the variable *total_precipitation* for the period October 2019 to May 2022. For both products, we extracted time series of daily precipitation for the grid point closest to the location of the lake outlet or the AWS (Figs. 1 and 3).

Our observational record is very short (<2.5 years). In order to discuss whether the observed patterns are persistent on a climatological scale (30 years), we also investigated ERA5-Land reanalysis data from 1993 to 2022 of both monthly precipitation and trajectory of moisture parcels over the region of Nepal and Tibet.

4 Results and discussion

4.1 Hydrological cycle of Golojang Co

Golojang Co water level has a strong seasonal cycle with an amplitude of approximately 70-80 cm (Fig. 2 - a). The lake level appears to plateau at low values from late winter (February) to pre-monsoon (April), several months after freeze-up in December, as it approaches the local hydrological base level (the minimum height at the lake outlet). The water temperature increases from 1 - 2 °C to a maximum of 6 °C in September. The increase in lake level and temperature is linked to the larger water input when the catchment unfreezes and when the monsoon brings most of the annual precipitation (Lei et al., 2018).

Golojang Co seasonal level cycle is more pronounced than the cycle of Paiku Co (Lei et al., 2021). ~~Paiku Co level During 2013 to 2017, Paiku Co water level had an average amplitude of 51 cm, and had a near constant decrease rate of 7 cm month⁻¹ during the post monsoon and the winter on average. Paiku Co level rises sharply at the end of pre-monsoon (Lei et al., 2018), but its level decreases slower than Golojang Co during post-monsoon and winter (Lei et al., 2021). It is difficult to compare these lakes, because Golojang Co has an outlet, whereas Paiku Co is the sink of the basin (endorheic lake with no outlet). Evaporation is thus the only loss term for Paiku Co whereas Golojang Co experiences drainage, with a decrease rate greater than 23 cm month⁻¹ during 2021 and 2022, and a much lower rate of 4 cm month⁻¹ during the winter.~~

125 4.2 Precipitation estimates from Golojang Co pressure time series

Using the Golojang Co pressure time series, we are able to observe 3 winters' snowfall at this previously unobserved site that lies between Yala and Paiku. We assess the conditions to apply Pritchard et al. (2021)'s method, which requires that precipitation falling in the lake catchment surrounding the lake does not run off into the lake but is stored as snow in freezing conditions. As a proxy indicator of a frozen catchment, we monitored the extent of ice cover on the lake surface and estimate the air temperature around the lake. The ice coverage percentage is known for 375 days, distributed between 20 September 2019 and 10 May 2022 (one image each 2.57 days in average). Golojang Co was at least 90% frozen during 250 of these days (Fig. 2 - a). During the hydrological years 2019 - 2020 and 2020 - 2021, the lake is partially frozen from the beginning of December to the beginning of July, lasting for 7 months each year. The catchment is in a frozen state (i.e., the lake is at least 90% frozen and air temperature is below zero at the lake elevation) from late December to mid-June. The precipitation from lake pressure could thus be estimated for winter and pre-monsoon (DJFMAM).

The total precipitation have been estimated to 420 ± 46 mm for the period 01 December 2019 to 31 May 2020, 307 ± 27 mm for the period 01 December 2020 to 31 May 2021, and 211 ± 9 mm for the period 01 December 2021 to 14 April 2022 (Fig. 3 - a, b and c). Two major events that happened on 21 May 2021 and 22 March 2022 were excluded from the cumulative DJFMAM snowfalls because we suspect possible presence of surface runoff around the lake due to the high temperatures recorded at these times in the catchment. These values are probably underestimated since the events identified on the pressure time series are mostly wet spells lasting on average 73 hours. One could hypothesize that the lack of short-duration snowfalls recorded at Golojang Co is due to the strong noise on the signal and on the rolling average applied on it that could mask small pressure variations (see discussion below).

Since no detailed study has been performed on Golojang Co before, there is only little or no knowledge about it, in particular none about its bathymetry. There is also no data about the interface between the lakes and the glaciers with which it is in contact. There is no quantitative data allowing us to estimate the impact of the calving on the pressure of the lake, but we note that calving events are abrupt, adding mass almost instantaneously to a proglacial lake. This contrasts with the slower and more sustained signal of water-pressure change from snowfall events that typically last for hours to days (Pritchard et al., 2021). Furthermore, visual inspection of satellite images show very limited calving events on the frozen lake during the period of study.

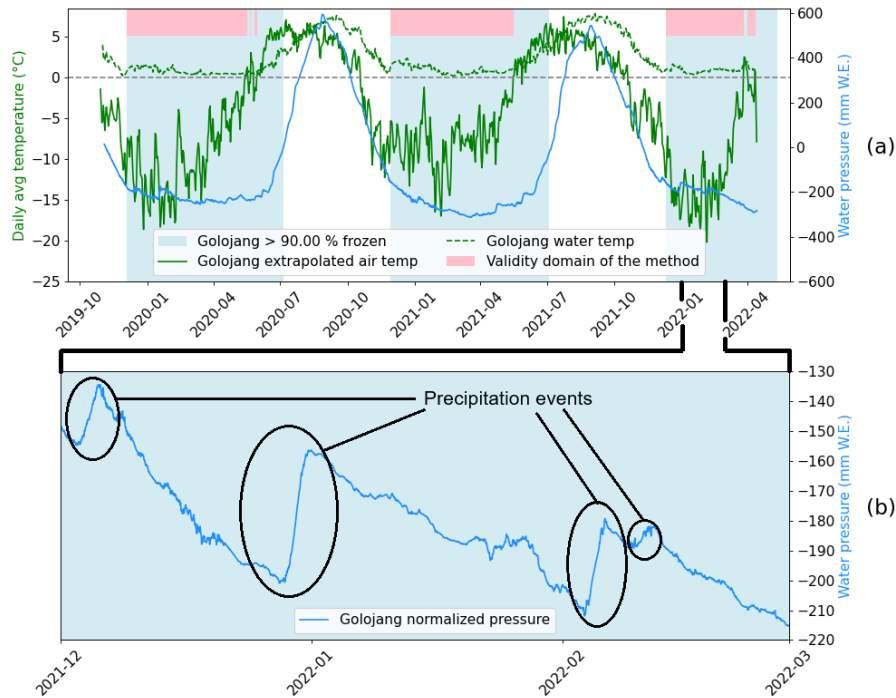


Figure 2. Water and extrapolated air temperature, validity domains of Pritchard et al. (2021)’s method and normalized pressure of Golojang from 31 November 2019 to 14 April 2022. Some examples of precipitation events on the pressure time series are highlighted on the bottom figure.

4.3 Measured precipitation at the automatic weather stations

When the time series overlap, we are able to compare the Golojang winter snowfall totals to those from the Yala and Paiku AWS. During DJFMAM 2019 - 2020 (Fig. 3 a, b and c), Paiku AWS recorded only 35 mm (9% of the total precipitation at Golojang Co for the same period). The Yala base camp AWS started recording during pre-monsoon 2020, therefore 2020 - 2021 is the only meteorological year with complete data. The Yala AWS recorded a total precipitation of 289 mm during winter and pre-monsoon, while Paiku AWS only recorded 25 mm. This corresponds to 94% and 8% of the total snowfalls at Golojang Co during the same period respectively. 226 mm of precipitation fell between 01 December 2021 and 14 April 2022 at Yala, but there was only 12 mm of precipitation at Paiku AWS, which corresponds respectively to 107% and 6% of the total snowfalls at Golojang for the same period.

160 While the Yala and Golojang Co snowfall observations are similar, the much lower precipitation totals recorded at Paiku AWS have the same order of magnitude as the precipitation-150 mm – 200 mm precipitation previously measured close to Paiku Co (Lei et al., 2018), located 25 km to the north, meaning that the winter and pre-monsoon precipitation in the southern and highest part of Paiku Co catchment is about ten times larger than in the lowest part of the catchment. Moreover, the transition gradient is very sharp, because Paiku AWS and Golojang Co are located only 10 km away, and Golojang Co is only 350 m

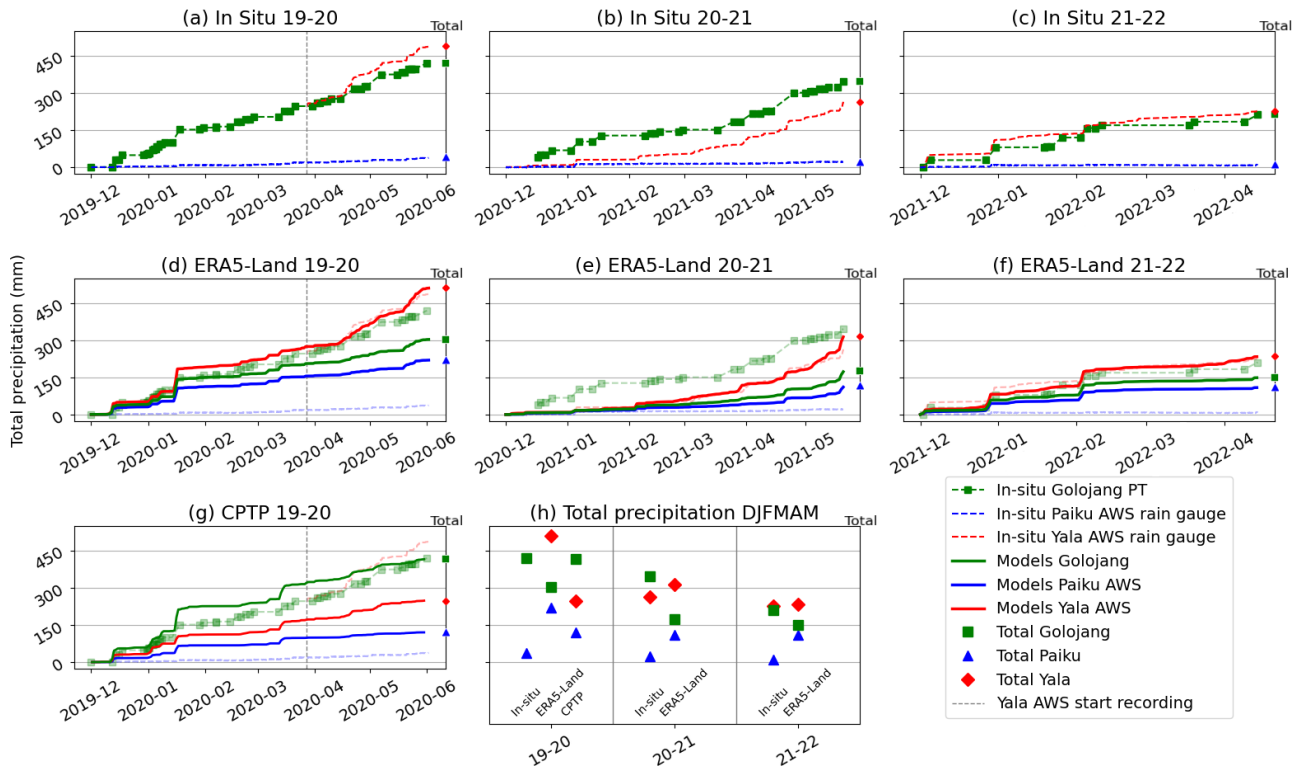


Figure 3. In-situ and model precipitation at the lake and both AWS locations. We note that the CORDEX FPS CPTP simulations are only available for the hydrological year of 19-20. Since Yala AWS started recording in April 2020, we choose to set its initial value to the same as in-situ Golojang during the middle of the year. The total cumulative precipitation for each period is shown on the right-hand bar of each graph and is summarized in (h).

165 higher than Paiku AWS. A large part of the major snowfall events seems to happen simultaneously at both Yala and Golojang
 with a similar intensity (Fig. 3 a, b and c)). Most of the events happen at Paiku AWS too, but with much reduced intensity.

Both AWS were equipped with wind shields. However, both gauges probably suffer from large undercatchment of snow
 since they are located in windy areas. Their respective anemometers recorded that the average wind speed during snowfall in
 Yala is about 2.3 m s^{-1} with a 0.8 quantile of 2.7 m s^{-1} while the average wind speed during a snowfall in Paiku is about
 170 5.9 m s^{-1} with a 0.8 quantile of 7.2 m s^{-1} . In order to asses the impact of the wind on the Paiku AWS recording, we computed
 the ratio of Paiku AWS precipitation recorded on Golojang precipitation estimation for events with average wind speeds below
 quantile 0.2 (4.4 m s^{-1}) and above quantile 0.8, for a total of 11 events each time. In the end, we have a ratio of 28% when
 the wind is weak ($<q 0.2$) and 18% when it is strong ($>q 0.8$). Although it is impossible to determine precisely what is due
 175 to undercatchment and what is due to meteorological effects, it is noticeable that the most extreme winds recorded induce a
 variation of only 10% of the ratio, making the precipitation estimated at Golojang Co still an order of magnitude above the
 precipitation at the Paiku AWS.

Although the strong winds in Paiku certainly induced a large undercatchment of snowfalls, the order of magnitude of the precipitation at the AWS is in any case an order of magnitude below the precipitation at Golojang Co.

4.4 Precipitation from reanalysis and atmospheric models

180 Both ERA5-Land and CPTP strongly overestimate the precipitation at Paiku AWS. ERA5-Land cumulative DJFMAM precipitation is, on average, 11 times larger than the in situ recording (Fig. 3 - d, e and f). CPTP is slightly closer to measurements by being only 3.4 times greater (Fig. 3 - g). The undercatch of the precipitation gauge cannot explain such a large difference. In addition, the precipitation computed by the models are far greater than the 15-30 mm winter precipitation estimated from previous studies (Lei et al., 2021, 2018).

185 ERA5-Land has a very good estimation of the cumulative DJFMAM ~~snowfalls precipitation~~ in Yala since the in situ is, on average, ~~1.08 times only 8%~~ greater than the ~~model AWS~~ during 2020-2021 and 2021-2022 (Fig. 3 - e and f). Unfortunately, Yala AWS was not working during ~~the only most of the~~ year of the CPTP simulation. ~~Nonetheless, since the in situ recording of the precipitation at the Yala AWS (241 mm, and completely missed winter precipitation as it started recording from 27 March 2020. For the period with recording (from 27 March 2020 to 31 May 2020) has the same order of magnitude as the estimation of ERA5-Land (468 mm during the same period, Yala AWS recorded 241 mm of precipitation (Fig. 3 - d), one could notice both sources of data have nearly the same estimate of cumulative precipitation at this location during the winter and the pre-monsoon. Compared to this, the a), against 76 mm estimation of CPTP would be a significant underestimation compared to ERA5-Land estimated by CPTP, which is a large underestimation~~ (Fig. 3 - g). Finally

190 ~~At Golojang Co, CPTP provides a DJFMAM cumulative snowfall estimate at Golojang Co that differs from the PT estimation by only 1.2% during 2019 - 2020, even though although CPTP slightly overestimates precipitation at the beginning of the study period and underestimates precipitation at the end compared to in situ (Fig. 3 - g). ERA5-Land shows much lower precipitation at Golojang Co, with PT estimates being on average 12.3 times 1230% greater for the three years (Fig. 3 - d, e, and f). However, Golojang in-situ estimates-~~

195 ~~At Golojang Co, CPTP provides a DJFMAM cumulative snowfall estimate at Golojang Co that differs from the PT estimation by only 1.2% during 2019 - 2020, even though although CPTP slightly overestimates precipitation at the beginning of the study period and underestimates precipitation at the end compared to in situ (Fig. 3 - g). ERA5-Land shows much lower precipitation at Golojang Co, with PT estimates being on average 12.3 times 1230% greater for the three years (Fig. 3 - d, e, and f). However, Golojang in-situ estimates-~~

200 ~~Although we use Golojang PT estimates as references here, they~~ are likely underestimated, as the pressure time series primarily captured wet spells averaging 73 hours, while shorter snowfalls may have been masked by ~~signal~~ noise. For comparison, during the period from 01 December 2020 to 31 May 2021 (the only complete meteorological year during which all sensors were working), there ~~was were~~ 26 events recorded at Yala ~~AWS site~~ by the AWS, of which 18 lasted less than 2 days and had an accumulation ~~of~~ less than 10 mm ~~of snow~~. At Golojang, the pressure time series allowed us to identify 23 events in the same period, of which only 7 could be matched with Yala ~~small~~ events.

205 4.5 Spatial distribution of precipitation

ERA5-Land and CPTP simulations show different patterns of DJFMAM precipitation over the southern Paiku Co basin and the northern Langtang national park. Due to the finer grid resolution, CPTP models can have the ability to better capture the influence of the complex terrain on precipitation patterns than ERA5-Land (Collier et al., 2024). In this study area CPTP models have a larger spatial variability than ERA5-Land. In particular, they show relatively high precipitation on the highest

210 parts of the study area, mainly above 5000 m a.s.l., and on the southern slopes of the Himalayas, as expected for orographic precipitation (Roe, 2005). In contrast, ERA5-Land predicts a relatively smooth precipitation gradient, with DJFMAM precipitation decreasing from southwest towards northeast (Fig. 1 - b and c).

Our spatially limited in situ observations, and the short duration of CPTP runs (one year), do not ~~allow~~-allows to conclude whether CPTP models or ERA5-Land reanalysis simulate a better distribution and amount of winter precipitation on the southern edge of the Tibetan plateau. Still, the ability of CPTP models to simulate sharp precipitation gradients over short distances is promising because our results suggest that such gradients can exist. Previous studies demonstrated that high resolution modeling can present large positive biases (He et al., 2019). More in situ recordings are still needed to determine whether the large gradients in CPTP product around the study area are realistic or exaggerated, although in situ observation networks are never perfectly fitted to evaluate model precipitation.

220 4.6 Climatological analysis

Our results suggest non-negligible precipitation during DJFMAM at Golojang Co, and thus could contribute more to glacier accumulation than previously extrapolated from ERA5-Land and AWS located on Paiku Co catchment (Martin et al., 2023). As our method is applicable only during winter conditions, we cannot conclude whether there is such a sharp precipitation gradient during monsoon, or in other words such high precipitation during the wettest season. In order to investigate whether precipitation gradients are similar during monsoon, we can only rely on ERA5 and ERA5-Land reanalysis that cover a long record (at least thirty ~~year~~-years of data).

The ERA5-Land monthly precipitation from 1993 to 2023 ~~reveal~~-reveals a highly marked seasonal pattern, with precipitation at Paiku AWS being 0.5 - 0.6 times the precipitation at Yala AWS during the winter and slowly decreasing to 0.3 - 0.4 during the monsoon, then increasing back progressively ~~-(Fig. A2)~~. The ratio of the precipitation between Paiku AWS and Golojang Co does not vary much, with only 20% variation between its minimum in August and its maximum in April. The pattern of integrated water vapor flow over the entire column in ERA5 reanalysis is consistent with this observation: in winter and pre-monsoon, there is a strong, very homogeneous north/south gradient, while during the monsoon (JJA) the pattern is much more heterogeneous over Nepal ~~-(Fig. A1)~~. Such results could be interpreted as seasonal variations of the spatial distribution of the precipitation over the southern Tibetan Plateau and northern Nepal, with once again, a stronger precipitation gradient during winter and pre-monsoon.

5 Conclusions

In this communication, we studied the hydro-meteorology of the northern Langtang National Park in Nepal and the Southern Paiku Co basin in Tibet using in-situ and modeled data from conventional and ~~new~~-recent methods. Using Pritchard et al. (2021) ~~recent~~-method, we estimated the snowfalls over the proglacial lake Golojang from 12 December 2019 to 09 April 2022, in the southern part of Paiku Co basin during the period DJFMAM. With this method, we converted the pressure time series of the lake that were recorded into estimates of the cumulative snowfalls when the lake is frozen. However, ~~because of the strong~~

~~noise on the signals, it may be possible that some events were not detected because of their small magnitudes~~smaller events
may not have been detected because their signals were too weak compared to the measurement noise. Our results highlight the potential of lakes to be used as precipitation gauges, which is especially valuable in data-scarce regions.

245 The snowfalls over the lake were compared to the precipitation recorded by AWS located on the southern side of the Himalaya (Yala Peak AWS in Langtang National Park) and on the Paiku Co catchment. During the three years of recording, it seems that Golojang Co cumulative ~~snowfalls during DJFMAM are~~snowfall during DJFMAM (200–400 mm) is closer to Yala AWS ~~, with a value of 200–400 mm,~~ than to Paiku AWS Co (5–35 mm)~~despite it is located much closer to the lake,~~
despite its proximity to Paiku Co.

250 We compared our results with precipitation data computed by reanalysis and atmospheric models (ERA5-Land and CORDEX-FPS CPTP). Both products largely overestimate the precipitation inside the Paiku Co basin compared to the automatic weather stations' recordings and our estimates based on pressure variations. Still, CPTP estimates are consistent with the DJFMAM precipitation recorded at Golojang during the meteorological year 2019 - 2020. ERA5-Land DJFMAM cumulative precipitation ~~are is~~ surprisingly very close to the recording of Yala AWS.

255 The in-situ data we gathered are thus not matching any model at all three locations at once. However, CPTP shows the best ability to reproduce the spatial distribution of the precipitation as it is recorded between the lake and the AWS. On the other hand, ERA5-Land was not matching any of the precipitation ~~recording~~recorded in the Paiku Co basin.

An analysis of the long term precipitation was performed over the three sites using ERA5-Land data from 1993 to 2022. Even though we show that ERA5-Land is not the better fit for a study on such a scale, it revealed a seasonal variation of the
260 spatial distribution of the precipitation, with a stronger gradient between Yala and the Paiku basin during the coldest part of the year (Dec. to May). This analysis suggests that we cannot extend our findings about precipitation gradients outside the cold season, due to different moisture ~~origin~~origins and circulation systems.

Code and data availability. The code used to calculate precipitation and its uncertainties can be accessed together with the event dates and Golojang Co pressure time series at <https://doi.org/10.5281/zenodo.14894770>, (Biget, 2025)

265 **Appendix A**

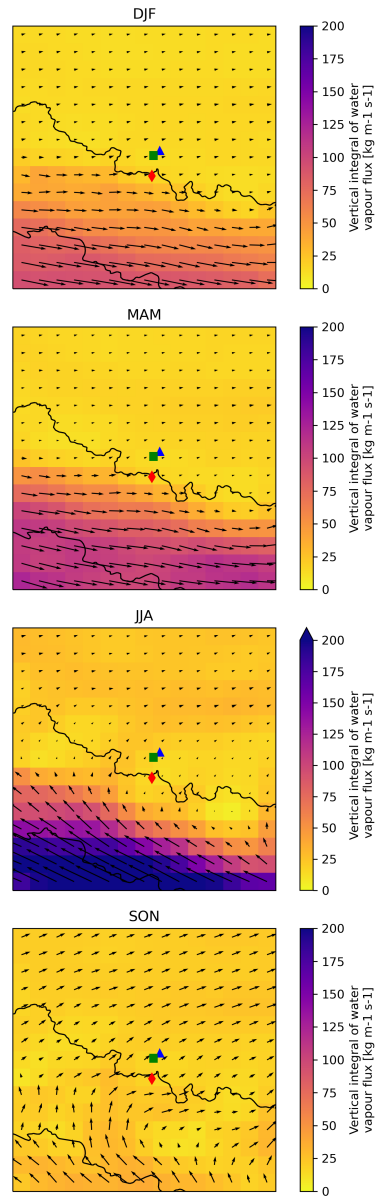


Figure A1. Vertical integral of water vapor flux from ERA5 reanalysis for the period 1993-2023. The red diamond shows the location of Yala AWS, the green square Golojang Co and the blue triangle Paiku AWS.

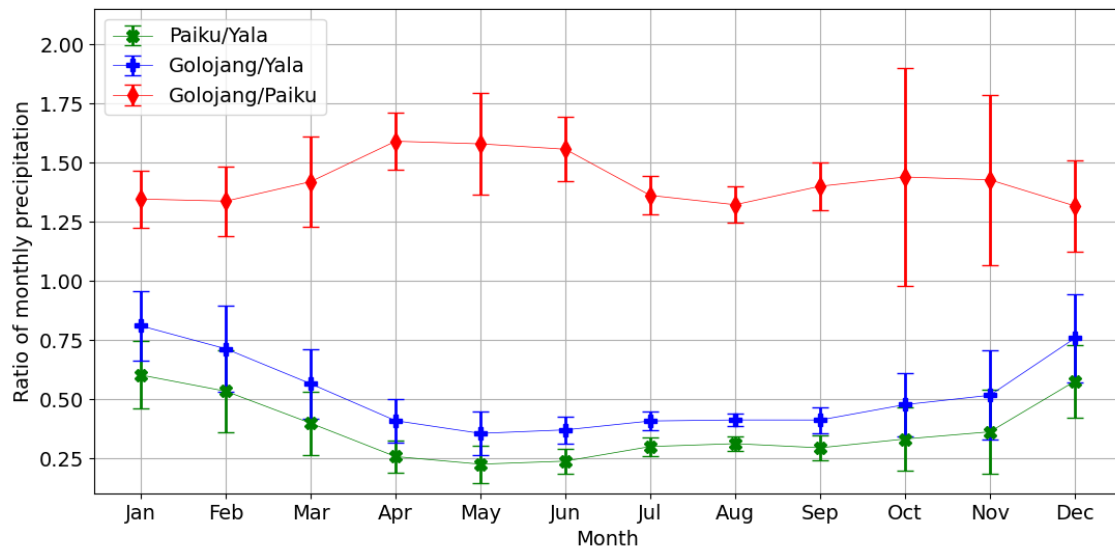


Figure A2. Ratios of mean monthly precipitation between different locations (Paiku/Yala, Golojang/Yala, Golojang/Paiku), calculated from ERA5-Land data for the period 1992–2021. Each point represents the mean ratio for a given month, and the error bars indicate ± 1 standard deviation of monthly precipitation over the 30-year period

Author contributions. Conceptualization: TB, FB, LM and WI; Data Curation: TB (lake pressure data), YL (lake pressure and meteorological data) and EC (CORDEX-FPS-CPTP data); Formal Analysis: TB; Funding Acquisition: WI and TY; Methodology: HP; Supervision: FB, LM and WI; Writing: all authors

Competing interests. Emily Collier is a member of the editorial board of The Cryosphere.

270 *Acknowledgements.* Leo Martin is funded by “Chaire de professeur junior” ENV DYN from the French Ministry of Research.

References

- Collier, E., Ban, N., Richter, N., Ahrens, B., Chen, D., Chen, X., Lai, H.-W., Leung, R., Li, L., Medvedova, A., Ou, T., Pothapakula, P. K., Potter, E., Prein, A. F., Sakaguchi, K., Schroeder, M., Singh, P., Sobolowski, S., Sugimoto, S., Tang, J., Yu, H., and Ziska, C.: The first ensemble of kilometer-scale simulations of a hydrological year over the third pole, *Climate Dynamics*, <https://doi.org/10.1007/s00382-275 024-07291-2>, 2024.
- Copernicus Climate Change Service: ERA5-Land hourly data from 1950 to present. Copernicus Climate Change Service (C3S) Climate Data Store (CDS), (Accessed on 02-Aug-2024), <https://doi.org/10.24381/cds.e2161bac>, 2022.
- Goodison, B. E., Louie, P. Y., and Yang, D.: WMO solid precipitation measurement intercomparison, 1998.
- He, C., Chen, F., Barlage, M., Liu, C., Newman, A., Tang, W., Ikeda, K., and Rasmussen, R.: Can Convection-Permitting Modeling Provide Decent Precipitation for Offline High-Resolution Snowpack Simulations Over Mountains?, *Journal of Geophysical Research: Atmospheres*, 124, 12 631–12 654, <https://doi.org/https://doi.org/10.1029/2019JD030823>, 2019.
- Immerzeel, W. W., Petersen, L., Ragetti, S., and Pellicciotti, F.: The importance of observed gradients of air temperature and precipitation for modeling runoff from a glacierized watershed in the Nepalese Himalayas, *Water Resour. Res.*, 50, 2212–2226, <https://doi.org/10.1002/2013wr014506>, 2014.
- 285 Kochendorfer, J., Nitu, R., Wolff, M., Mekis, E., Rasmussen, R., Baker, B., Earle, M. E., Reverdin, A., Wong, K., Smith, C. D., Yang, D., Roulet, Y.-A., Buisan, S., Laine, T., Lee, G., Aceituno, J. L. C., Alastrué, J., Isaksen, K., Meyers, T., Brækkan, R., Landolt, S., Jachcik, A., and Poikonen, A.: Analysis of single-shielded and unshielded measurements of mixed and solid precipitation from WMO-SPICE, *Hydrology and Earth System Sciences*, 21, 3525–3542, <https://doi.org/10.5194/hess-21-3525-2017>, 2017.
- Lea, J.: The Google Earth Engine Digitisation Tool (GEEDiT) and the Margin change Quantification Tool (MaQiT) – Simple tools for the rapid mapping and quantification of changing Earth surface margins, *Earth Surface Dynamics*, 6, 551–561, <https://doi.org/10.5194/esurf-290 6-551-2018>, 2018.
- Lei, Y., Yao, T., Yang, K., Bird, B. W., Tian, L., Zhang, X., Wang, W., Xiang, Y., Dai, Y., Lazhu, Zhou, J., and Wang, L.: An integrated investigation of lake storage and water level changes in the Paiku Co basin, central Himalayas, *Journal of Hydrology*, 562, 599–608, <https://doi.org/https://doi.org/10.1016/j.jhydrol.2018.05.040>, 2018.
- 295 Lei, Y., Yao, T., Yang, K., Lazhu, Ma, Y., and Bird, B. W.: Contrasting hydrological and thermal intensities determine seasonal lake-level variations – a case study at Paiku Co on the southern Tibetan Plateau, *Hydrology and Earth System Sciences*, 25, 3163–3177, <https://doi.org/10.5194/hess-25-3163-2021>, 2021.
- Martin, L., Westermann, S., Magni, M., Brun, F., Fiddes, J., Lei, Y., Kraaijenbrink, P., Mathys, T., Langer, M., Allen, S., and Immerzeel, W.: Recent ground thermo-hydrological changes in a southern Tibetan endorheic catchment and implications for lake level changes, *Hydrology and Earth System Sciences*, 27, 4409–4436, <https://doi.org/10.5194/hess-27-4409-2023>, 2023.
- 300 Muñoz Sabater, J., Dutra, E., Agustí-Panareda, A., Albergel, C., Arduini, G., Balsamo, G., Boussetta, S., Choulga, M., Harrigan, S., Hersbach, H., Martens, B., Miralles, D. G., Piles, M., Rodríguez-Fernández, N. J., Zsoter, E., Buontempo, C., and Thépaut, J.-N.: ERA5-Land: a state-of-the-art global reanalysis dataset for land applications, *Earth System Science Data*, 13, 4349–4383, <https://doi.org/10.5194/essd-13-4349-2021>, 2021.
- 305 Prein, A. F., Ban, N., Ou, T., Tang, J., Sakaguchi, K., Collier, E., Jayanarayanan, S., Li, L., Sobolowski, S., Chen, X., Zhou, X., Lai, H.-W., Sugimoto, S., Zou, L., Hasson, S. u., Ekstrom, M., Pothapakula, P. K., Ahrens, B., Stuart, R., Steen-Larsen, H. C., Leung, R., Belusic, D.,

- Kukulies, J., Curio, J., and Chen, D.: Towards Ensemble-Based Kilometer-Scale Climate Simulations over the Third Pole Region, *Climate Dynamics*, 60, 4055–4081, <https://doi.org/10.1007/s00382-022-06543-3>, 2023.
- 310 Pritchard, H. D., Farinotti, D., and Colwell, S.: Measuring Changes in Snowpack SWE Continuously on a Landscape Scale Using Lake Water Pressure, *Journal of Hydrometeorology*, 22, 795 – 811, <https://doi.org/10.1175/JHM-D-20-0206.1>, 2021.
- Roe, G. H.: OROGRAPHIC PRECIPITATION, *Annual Review of Earth and Planetary Sciences*, 33, 645–671, <https://doi.org/https://doi.org/10.1146/annurev.earth.33.092203.122541>, 2005.
- Yang, K., Wu, H., Qin, J., Lin, C., Tang, W., and Chen, Y.: Recent climate changes over the Tibetan Plateau and their impacts on energy and water cycle: A review, *Global and Planetary Change*, 112, 79–91, <https://doi.org/10.1016/j.gloplacha.2013.12.001>, 2014.
- 315 Zhang, G., Yao, T., Shum, C. K., Yi, S., Yang, K., Xie, H., Feng, W., Bolch, T., Wang, L., Behrangi, A., Zhang, H., Wang, W., Xiang, Y., and Yu, J.: Lake volume and groundwater storage variations in Tibetan Plateau’s endorheic basin, *Geophysical Research Letters*, 44, 5550–5560, <https://doi.org/10.1002/2017GL073773>, 2017.
- Zhang, G., Bolch, T., Chen, W., and Crétaux, J.-F.: Comprehensive estimation of lake volume changes on the Tibetan Plateau during 1976–2019 and basin-wide glacier contribution, *Science of The Total Environment*, 772, 145463, <https://doi.org/10.1016/j.scitotenv.2021.145463>, 2021.
- 320